

## LETTERS

# An endocannabinoid mechanism for stress-induced analgesia

Andrea G. Hohmann<sup>1</sup>, Richard L. Suplita<sup>1</sup>, Nathan M. Bolton<sup>1</sup>, Mark H. Neely<sup>1</sup>, Darren Fegley<sup>2</sup>, Regina Mangieri<sup>2</sup>, Jocelyn F. Krey<sup>3</sup>, J. Michael Walker<sup>3</sup>, Philip V. Holmes<sup>1</sup>, Jonathon D. Crystal<sup>1</sup>, Andrea Duranti<sup>4</sup>, Andrea Tontini<sup>4</sup>, Marco Mor<sup>5</sup>, Giorgio Tarzia<sup>4</sup> & Daniele Piomelli<sup>2</sup>

Acute stress suppresses pain by activating brain pathways that engage opioid or non-opioid mechanisms. Here we show that an opioid-independent form of this phenomenon, termed stress-induced analgesia<sup>1</sup>, is mediated by the release of endogenous marijuana-like (cannabinoid) compounds in the brain. Blockade of cannabinoid CB<sub>1</sub> receptors in the periaqueductal grey matter of the midbrain prevents non-opioid stress-induced analgesia. In this region, stress elicits the rapid formation of two endogenous cannabinoids, the lipids 2-arachidonoylglycerol<sup>2</sup> (2-AG) and anandamide<sup>3</sup>. A newly developed inhibitor of the 2-AG-deactivating enzyme, monoacylglycerol lipase<sup>4,5</sup>, selectively increases 2-AG concentrations and, when injected into the periaqueductal grey matter, enhances stress-induced analgesia in a CB<sub>1</sub>-dependent manner. Inhibitors of the anandamide-deactivating enzyme fatty-acid amide hydrolase<sup>6</sup>, which selectively elevate anandamide concentrations, exert similar effects. Our results indicate that the coordinated release of 2-AG and anandamide in the periaqueductal grey matter might mediate opioid-independent stress-induced analgesia. These studies also identify monoacylglycerol lipase as a previously unrecognized therapeutic target.

Stress activates neural systems that inhibit pain sensation. This adaptive response, referred to as stress-induced analgesia (SIA), depends on the recruitment of brain pathways that project from the amygdala to the midbrain periaqueductal grey matter (PAG) and descend to the brainstem rostroventromedial medulla and dorsal horn of the spinal cord<sup>7</sup>. Endogenous opioid peptides have key functions in this process<sup>1,8</sup>, but other as yet unidentified neurotransmitters are also known to be involved<sup>1</sup>. We proposed that endocannabinoids might be implicated in stress analgesia for two reasons. First, agonists of CB<sub>1</sub> receptors—the predominant cannabinoid receptor subtype present in the brain<sup>9,10</sup>—exert profound antinociceptive effects<sup>7</sup> and suppress activity in nociceptive neurons<sup>11–14</sup>. Second, CB<sub>1</sub> antagonists increase the activity of nociceptive rostroventromedial medulla neurons<sup>14</sup> and enhance sensitivity to noxious stimuli<sup>15</sup>, indicating that an intrinsic endocannabinoid tone might regulate descending antinociceptive pathways<sup>7</sup>.

To study non-opioid SIA we delivered brief, continuous electric foot shock to rats and quantified their sensitivity to pain after stress by using the tail-flick test. As demonstrated previously<sup>1,16</sup>, this stimulation protocol caused a profound antinociceptive effect that was not affected by intraperitoneal (i.p.) injection of the opiate antagonist naltrexone (14 mg kg<sup>-1</sup>) (Fig. 1a). However, the response was almost abolished by administration of the CB<sub>1</sub> antagonist rimonabant (SR141617A, 5 mg kg<sup>-1</sup> i.p.) (Fig. 1a) or its analogue AM251 (5 mg kg<sup>-1</sup> i.p.) (Supplementary Fig. 1), but not by the CB<sub>2</sub>

antagonist SR144528 (5 mg kg<sup>-1</sup> i.p.) (Fig. 1a). The effects of CB<sub>1</sub> antagonists cannot be attributed to changes in basal nociceptive threshold because, in the absence of the stressor, the drugs failed to alter tail-flick latencies (Supplementary Figs 1 and 2).

If CB<sub>1</sub> activation is required for the expression of non-opioid SIA, the latter should be lower in animals rendered tolerant to the

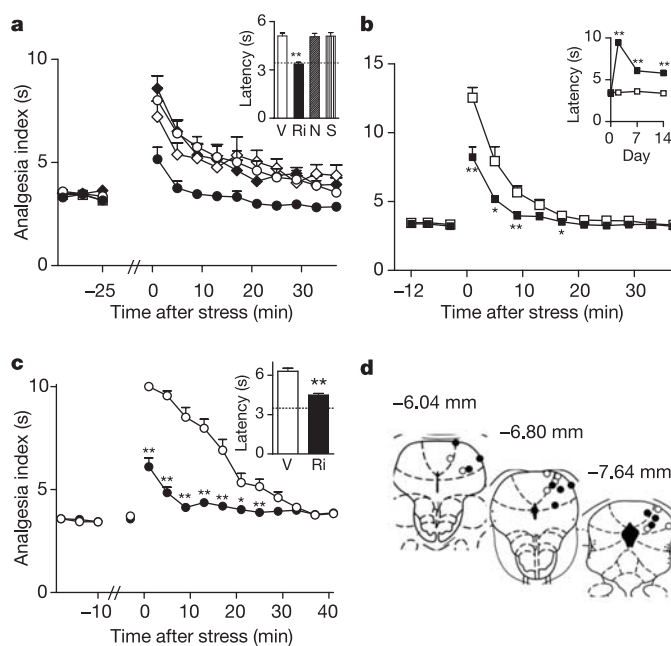


**Figure 1 | CB<sub>1</sub> receptors mediate non-opioid stress-induced analgesia.**

**a**, CB<sub>1</sub> antagonist rimonabant (Ri, filled circles) blocks stress antinociception. Opiate antagonist naltrexone (N, open diamonds) and CB<sub>2</sub> antagonist SR144528 (S, filled diamonds) have no effect. Open circles, vehicle (V). Inset: drug effects ( $F_{3,29} = 5.99$ ,  $P < 0.003$ ). The dotted line indicates the nociceptive threshold. Analgesia index was measured as the tail-flick latency. **b**, Stress antinociception is attenuated in WIN55212-2-tolerant rats (filled squares) compared with controls (open squares) ( $F_{1,19} = 16.74$ ,  $P < 0.0007$ ). Inset: non-stress cannabinoid antinociception is attenuated in WIN55212-2-tolerant rats ( $F_{2,38} = 35.11$ ,  $P < 0.0002$ ). **c**, Rimonabant in dorsolateral PAG suppresses stress antinociception ( $F_{10,170} = 20.01$ ,  $P < 0.0002$ ). Inset: drug effects ( $F_{1,17} = 25.63$ ,  $P < 0.0002$ ). **d**, PAG injection sites. Error bars, where visible, indicate s.e.m.;  $n = 6–11$  per group. Asterisk,  $P < 0.05$ ; two asterisks,  $P < 0.01$  (analysis of variance, Fisher's PLSD test).

<sup>1</sup>Neuroscience and Behavior Program, Department of Psychology, The University of Georgia, Athens, Georgia 30602-3013, USA. <sup>2</sup>Department of Pharmacology and Center for Drug Discovery, University of California, Irvine, California 92697-4260, USA. <sup>3</sup>Schriber Research Laboratory, Departments of Psychology and Neuroscience, Brown University, Providence, Rhode Island 02912, USA. <sup>4</sup>Institute of Medicinal Chemistry, University of Urbino Carlo Bo, I-61029 Urbino, Italy. <sup>5</sup>Pharmaceutical Department, University of Parma, I-43100 Parma, Italy.

antinociceptive effects of cannabinoids. Consistent with this prediction, rats chronically treated with the cannabinoid agonist WIN55212-2 (10 mg kg<sup>-1</sup> i.p., once daily for 14 days) displayed, along with the expected blunting of acute CB<sub>1</sub>-dependent antinociception (Fig. 1b, inset), a marked decrease in stress antinociception (Fig. 1b). The possibility that this decrement might be due to changes in opioid tone is unlikely for two reasons: first, rats tolerant to WIN55212-2 showed no deficit in their antinociceptive response to morphine (2.5 mg kg<sup>-1</sup> subcutaneously) (data not shown); and second, in accord with previous results<sup>16</sup>, rats tolerant to morphine (10 mg kg<sup>-1</sup> subcutaneously once daily for 7 days) showed normal non-opioid stress antinociception (Supplementary Fig. 3).

The PAG serves key functions in both the descending control of pain<sup>7,17</sup> and the antinociceptive actions of cannabinoid agonists<sup>18</sup>. We therefore asked whether blockade of CB<sub>1</sub> receptors in this structure could affect SIA. Rimonabant (2 nmol) reduced stress antinociception when microinjected into the dorsolateral PAG (Fig. 1c, d), a structure linked to non-opioid stimulation-produced analgesia<sup>17,19</sup>, but was inactive after injection into the lateral and ventrolateral PAG (Supplementary Fig. 4). The antagonist was also ineffective when administered into the lateral ventricle, indicating that its actions were not due to diffusion to distal sites (Supplementary Fig. 5). These results are consistent with the presence of CB<sub>1</sub> receptors throughout the dorsal midbrain<sup>9,20</sup> and indicate that endocannabinoid release and/or intrinsic CB<sub>1</sub> receptor activity in the PAG might contribute to SIA.

To determine whether endocannabinoid release participates in this response, we measured anandamide and 2-AG concentrations in the dorsal midbrain of rats killed before (nonshock) or at various times after foot shock (Supplementary Fig. 6). Liquid chromatography/mass spectrometry (LC-MS) analyses revealed that midbrain 2-AG concentrations were markedly increased 2 min after shock termination and returned to baseline about 15 min later (Fig. 2a). This response preceded a sustained increase in anandamide concentration, which

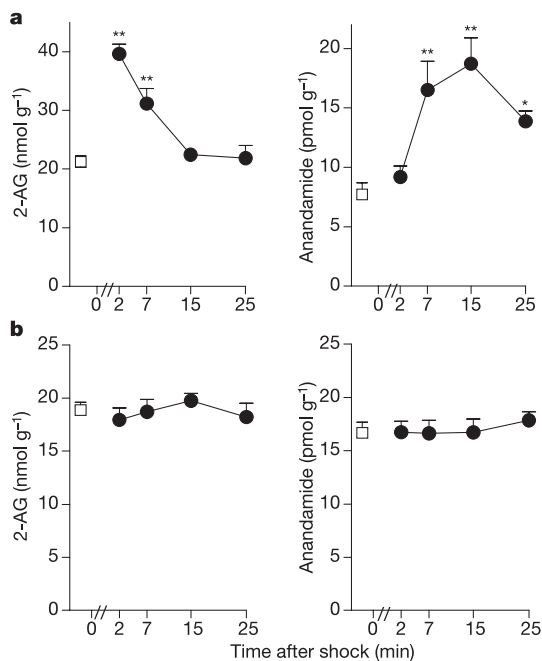


**Figure 2 | Stress stimulates the formation of 2-AG and anandamide in dorsal midbrain.** Non-stress (open squares) and post-stress (filled circles) concentrations of 2-AG and anandamide in dorsal midbrain samples containing the entire PAG (a) and in occipital cortex samples (b). Error bars indicate s.e.m.;  $n = 10$  per group. Asterisk,  $P < 0.05$  compared with non-stressed controls; two asterisks,  $P < 0.01$ .

peaked 7–15 min after foot shock (Fig. 2a). No such changes were observed in the occipital cortex (Fig. 2b), a brain region that contains CB<sub>1</sub> receptors<sup>9</sup> but is not considered part of the SIA circuit.

The rapid accumulation of 2-AG in the midbrain after stress indicates that endocannabinoid release, rather than intrinsic CB<sub>1</sub> activity, might be responsible for SIA. If this is so, selective inhibitors of the 2-AG-hydrolysing enzyme monoacylglycerol lipase (MGL) should heighten the intrinsic actions of 2-AG and enhance its analgesic effects. The absence of selective MGL inhibitors prompted us to develop such an agent. To develop MGL-specific inhibitors we started from the assumption that similarities should exist between the substrate-binding site of MGL and that of the anandamide-hydrolysing enzyme fatty-acid amide hydrolase (FAAH)<sup>6</sup>: the fact that both hydrolases cleave arachidonic-acid derivatives indicates that their binding pockets might accommodate inhibitors of similar bulk and hydrophobicity. We therefore examined a collection of carbamate derivatives in which selective FAAH inhibition had been achieved by mimicking the flexible acyl chain of anandamide with the isosteric, but more rigid, biphenyl group (Fig. 3a)<sup>21,22</sup>. This screening revealed that although *O*-biphenyl carbamates (Fig. 3a: 1, URB597; 2, URB524) inhibit the activity of FAAH but not that of MGL, *N*-biphenyl carbamates (Fig. 3a, 3, URB602) display an opposite selectivity (Fig. 3b, c). URB602 inhibited rat brain MGL with a half-maximal concentration (IC<sub>50</sub>) of  $28 \pm 4 \mu\text{M}$  (Fig. 3b) through a noncompetitive mechanism. Without URB602, the apparent Michaelis constant ( $K_m$ ) of MGL for 2-AG was  $24.0 \pm 1.7 \mu\text{M}$  and the maximum velocity ( $V_{max}$ ) was  $1814 \pm 51 \text{ nmol min per mg protein}$ ; with URB602, the  $K_m$  was  $20.0 \pm 0.4 \mu\text{M}$  and the  $V_{max}$  was  $541 \pm 20 \text{ nmol min per mg protein}$  ( $n = 4$ ). When organotypic slice

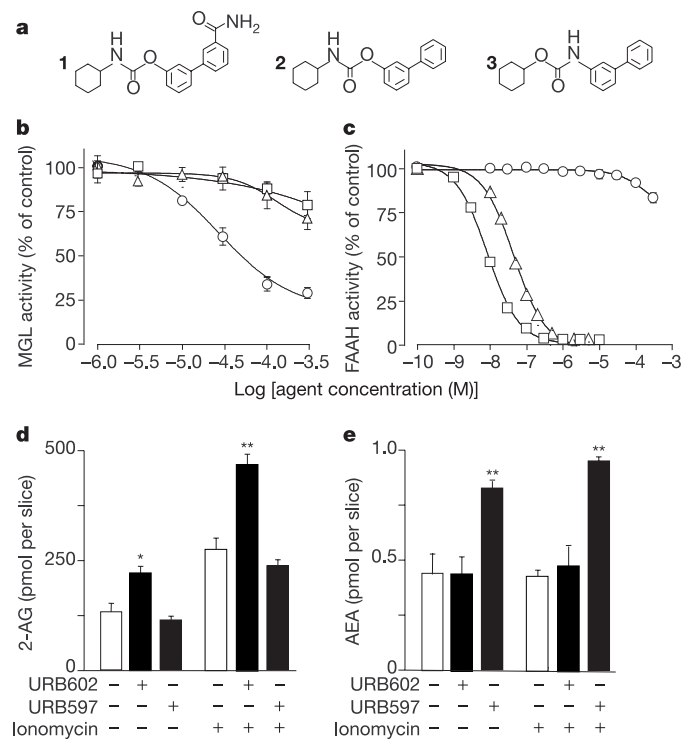


**Figure 3 | URB602 is a selective MGL inhibitor.** a, Structures of *O*-biphenyl-substituted FAAH inhibitors (1, URB597; 2, URB524) and the *N*-biphenyl-substituted MGL inhibitor URB602 (3). b, URB602 (circles) inhibits rat brain MGL activity, whereas URB597 (squares) and URB524 (triangles) have no such effect. c, URB602 does not affect rat brain FAAH activity, which is suppressed by URB597 and URB524. d, e, URB602 (100  $\mu\text{M}$ ) increases the concentration of 2-AG (d) but not of anandamide (e) in rat brain slice cultures. Effects of ionomycin (2  $\mu\text{M}$ ) and URB597 (1  $\mu\text{M}$ ) are also shown. Asterisk,  $P < 0.05$ ; two asterisks,  $P < 0.01$  versus control, *t*-test ( $n = 4$ ). Error bars indicate s.e.m.

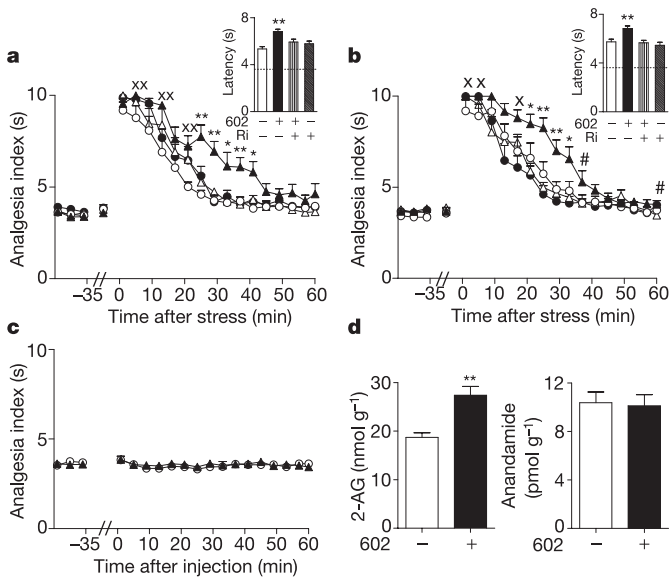


**Figure 4 | The MGL inhibitor URB602 enhances non-opioid stress-induced analgesia.** **a, b**, URB602 (602) increases stress antinociception when microinjected in dorsolateral PAG (**a**) and lateral/ventrolateral PAG (**b**), but does not cause antinociception in non-stressed rats (lateral/ventrolateral PAG) (**c**). Rimobant blocks these effects. Open circles, vehicle; filled triangles, URB602; filled circles, rimobant; open triangles, URB602/rimobant. Analgesia index was measured as the tail-flick latency. Insets: drug effects (**a**,  $F_{3,26} = 7.39$ ,  $P < 0.002$ ; **b**,  $F_{3,25} = 9.15$ ,  $P < 0.0004$ ). Dotted lines indicate nociceptive thresholds. **d**, URB602 in the ventrolateral PAG increases the concentration of 2-AG, but not of anandamide, measured 25 min after shock. Error bars indicate s.e.m.;  $n = 6-10$  per group. Asterisk,  $P < 0.05$  compared with all groups; two asterisks,  $P < 0.01$ ; cross,  $P < 0.05$  compared with vehicle; two crosses,  $P < 0.01$ ; hash,  $P < 0.05$  compared with URB602/rimobant; ANOVA, Fisher's PLSD post-hoc test.

cultures of rat forebrain were incubated with URB602 (100  $\mu\text{M}$ ), both baseline and  $\text{Ca}^{2+}$ -ionophore-stimulated 2-AG concentrations were increased (Fig. 3d). In contrast, URB602 did not change anandamide content (Fig. 3e), which was markedly elevated by the FAAH inhibitor URB597 (ref. 21) at 1  $\mu\text{M}$  (Fig. 3e). Moreover,

URB602 did not affect the activities of lipid-metabolizing enzymes such as diacylglycerol lipase<sup>23</sup> and cyclooxygenase-2 (ref. 24) and did not significantly influence binding of [<sup>3</sup>H]WIN55212-2 to CB<sub>1</sub> or CB<sub>2</sub> receptors ( $\text{IC}_{50} \geq 5 \mu\text{M}$ ) or [<sup>35</sup>S]GTP- $\gamma$ S to rat cerebellar membranes (half-maximal effective concentration ( $\text{EC}_{50}$ ) > 50  $\mu\text{M}$ ) (Supplementary Table 1, and data not shown).

Because of its relatively low potency, URB602 is not suitable for systemic administration. Nevertheless, microinjections of the MGL inhibitor (0.1 nmol) into the dorsolateral PAG (Supplementary Fig. 7a) or lateral/ventrolateral PAG (Supplementary Fig. 7b) enhanced stress-induced antinociception (Fig. 4a, b). Basal nociceptive thresholds in non-shocked rats were unaffected (Fig. 4c; Supplementary Fig. 7c). This effect was probably due to the accumulation of 2-AG in the PAG, for three reasons. First, it was prevented by the simultaneous administration of rimobant (0.2 nmol) (Fig. 4a, b). Second, it was mimicked by the non-selective MGL inhibitor methyl arachidonyl fluorophosphate<sup>5</sup> (2.6 nmol), whose effects also were blocked by rimobant (Supplementary Fig. 9). Last, it was accompanied by an increase in midbrain 2-AG concentration: 25 min after foot shock, when the antinociceptive effect of URB602 was at its peak (Fig. 4a, b), 2-AG content was significantly higher in midbrain fragments of URB602-treated rats relative to vehicle-treated controls (Fig. 4d). Anandamide concentrations were identical in the two groups (Fig. 4d), further highlighting the selectivity of URB602 for MGL. These results indicate that URB602 is a selective MGL inhibitor that enhances stress antinociception.

To examine the possible role of anandamide in SIA, we administered the FAAH inhibitor URB597 (ref. 21) either by systemic (0.3 mg  $\text{kg}^{-1}$ , i.p.) (Fig. 5a) or local (0.1 nmol) (Fig. 5b; Supplementary Fig. 8) injection into the dorsolateral PAG. In both cases URB597 caused a potentiation of stress antinociception, which was prevented by rimobant (1 mg  $\text{kg}^{-1}$  i.p.; 0.2 nmol in the PAG) (Fig. 5a, b). The FAAH inhibitor did not modify basal nociceptive thresholds (Fig. 5a, b). Furthermore, administration of the anandamide transport inhibitor VDM11 (10 mg  $\text{kg}^{-1}$  i.p.)<sup>25</sup> exerted similar effects, which also were blocked by rimobant (2 mg  $\text{kg}^{-1}$  i.p.) (Fig. 5c).

Our results indicate that the concerted release of 2-AG and anandamide in the PAG might mediate non-opioid SIA. The two endocannabinoids might act on local CB<sub>1</sub> receptors<sup>9,20,26</sup> to regulate

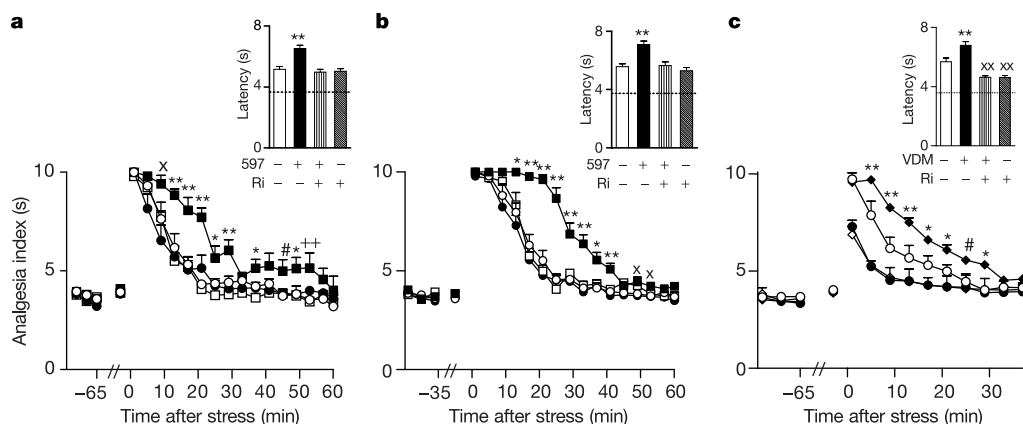


**Figure 5 | Inhibitors of anandamide hydrolysis (URB597) and transport (VDM11) enhance non-opioid stress-induced analgesia.** URB597 (filled squares) administered systemically (**a**) or in dorsolateral PAG (**b**) and VDM11 (filled diamonds) administered systemically (**c**) potentiate stress antinociception. Rimobant blocks these effects after systemic administration (**a**, 1 mg  $\text{kg}^{-1}$ ; **c**, 2 mg  $\text{kg}^{-1}$ ) or administration in PAG (**b**). Vehicle, open circles; rimobant, filled circles, URB597/rimobant, open squares; VDM11/rimobant, open diamonds. Analgesia index was

measured as the tail-flick latency. Insets: effects of URB597 (**a**,  $F_{3,28} = 11.56$ ,  $P < 0.0002$ ; **b**,  $F_{3,24} = 33.69$ ,  $P < 0.0002$ ) and VDM11 (**c**,  $F_{3,26} = 21.76$ ,  $P < 0.0002$ ). Error bars indicate s.e.m.;  $n = 5-9$  per group. Asterisk,  $P < 0.05$  compared with all groups; two asterisks,  $P < 0.01$ ; cross,  $P < 0.05$  compared with vehicle; two crosses,  $P < 0.01$ ; hash,  $P < 0.05$  compared with rimobant (ANOVA, Fisher's PLSD post-hoc test). Dotted lines indicate nociceptive thresholds.

glutamate- and GABA-mediated transmission, ultimately disinhibiting descending pain control pathways. Three points are noteworthy. First, endocannabinoid-dependent stress antinociception is not affected by opioid antagonists or morphine tolerance, implying that it might not require opioid activity. The reverse may not be true, however, because mutant CB<sub>1</sub>-null mice have reduced opioid-mediated responses to stress<sup>27</sup>. Second, the residual antinociception observed in the presence of CB<sub>1</sub> antagonists leaves open the possibility that additional mediators of SIA remain to be discovered. Last, stress triggers the formation of both 2-AG and anandamide in the midbrain, but these two endocannabinoids are released with strikingly dissimilar time-courses. This observation underscores the existence of functional differences between these signalling molecules<sup>28</sup>, pointing to the possibility that they might act in a coordinated manner to modulate temporally and/or spatially distinct processes in the PAG and other brain regions. The ability of both MGL and FAAH inhibitors to magnify endocannabinoid-dependent SIA also highlights the significance of these enzymes as previously undescribed targets for the treatment of pain and stress-related disorders.

## METHODS

**Chemicals.** We synthesized URB597, URB524 and [<sup>2</sup>H<sub>4</sub>]anandamide as described<sup>21,22,29,30</sup>, and URB602 (biphenyl-3-yl carbamic acid cyclohexyl ester) by reacting diimidazole-1-ylmethanone with biphenyl-3-yl amine in acetonitrile in the presence of 4-dimethylaminopyridine and subsequently with cyclohexanol. Other chemicals were obtained and administered as described in Supplementary Methods.

**Animals.** We used adult male Sprague–Dawley rats for *in vivo* experiments and Wistar rats for enzyme assays and tissue cultures. All procedures were approved by the institutional animal care and use committee and followed guidelines of the International Association for the Study of Pain.

**Brain slice cultures.** We cultured brain slices from Wistar rats. Pups were killed on postnatal day 5 by decapitation after cryo-anaesthesia. Brains were removed and cut (0.4-mm-thick coronal slices) with a vibratome in a bath of ice-cold high-glucose DMEM (Gibco). Hemispheres were placed on Millicell culture inserts (Millipore) in six-well plates with serum-based culture medium (1.5 ml) composed of basal Eagle's medium with Earle's salts (100 ml), Earle's balanced salt solution (50 ml), heat-inactivated horse serum (50 ml), L-glutamine (0.2 mM, 1 ml) and 50% glucose (2 ml) (all from Gibco). Slices were maintained at 37°C with 5% CO<sub>2</sub> for 7 days before use.

**Lipid extractions and LC–MS analyses.** For *ex vivo* experiments, we habituated rats to the guillotine for at least 7 days before the experiment and killed them either before or at various times (2, 7, 15 and 25 min) after a 3-min foot shock (*n* = 10 per group). The brains were rapidly removed, dissected and stored frozen (–80°C) until lipid extraction. For *in vitro* experiments, we removed the medium of slice cultures and replaced it with DMEM (1 ml) containing URB602 (100 μM), URB597 (1 μM) or vehicle (0.1% dimethylsulphoxide) and incubated the slices at 25°C for 10 min. In some experiments, slices were incubated with ionomycin (2 μM) in DMEM for a further 15 min. Reactions were stopped and washed with ice-cold 50% methanol (1 ml). Slices were collected in the same medium (0.2 ml) and homogenized. Brain tissue (about 50 mg) and slice homogenates were suspended in methanol (2 ml) including <sup>2</sup>H-containing internal standards (25 pmol). Lipids were extracted in methanol/chloroform/water (1:2:0.25). The organic phase was recovered, evaporated to dryness, reconstituted in chloroform/methanol (1:3, 80 μl) and subjected to LC–MS analysis as described<sup>30</sup>.

**Enzyme assays.** We prepared cell fractions from Wistar rat brain homogenates, and assayed cytosol MGL activity and membrane FAAH activity with 2-monooleoyl[1,2,3-<sup>3</sup>H]glycerol (ARC; 20 Ci mmol<sup>-1</sup>), and [ethanolamine-<sup>3</sup>H]anandamide (ARC; 60 Ci mmol<sup>-1</sup>), respectively, as substrates<sup>4,21</sup>.

**Surgery and tolerance induction.** We implanted stainless-steel guide cannulae in the PAG (dorsolateral or lateral/ventrolateral) or left lateral ventricle under pentobarbital/ketamine anaesthesia 3–7 days before testing. Placements of cannulae were verified in Nissl-stained sections or by post-mortem injection of fast green dye. Analyses were restricted to animals exhibiting dye spread throughout the ventricular system. The induction of tolerance to WIN55212-2 and morphine is described in Supplementary Methods.

**Assessment of antinociception.** We administered foot shock (0.9 mA, alternating current, for 3 min) to Sprague–Dawley rats with a Lafayette grid-shock apparatus. Withdrawal latencies in the radiant-heat tail-flick test<sup>13,17</sup> were measured at 2-min intervals before (baseline) and after foot shock, and calculated for each subject in two-trial blocks. Removal of the tail from the

heat source terminated the application of thermal stimulation. Tail-flick latencies were monitored for 4 min immediately before exposure to the stressor to evaluate changes in nociceptive thresholds induced by pharmacological manipulations. Ceiling tail-flick latencies were 10 s except where noted. Tail-flick latencies, measured at baseline or before administration of the stressor, did not differ between groups in any study.

**Data analyses.** We analysed results with analysis of variance (ANOVA), repeated-measures ANOVA and Fisher's protected least-significant-difference post-hoc tests. *P* < 0.05 was considered significant.

Received 23 February; accepted 18 April 2005.

- Lewis, J. W., Cannon, J. T. & Liebeskind, J. C. Opioid and nonopioid mechanisms of stress analgesia. *Science* **208**, 623–625 (1980).
- Mechoulam, R. *et al.* Identification of an endogenous 2-monoglyceride, present in canine gut, that binds to cannabinoid receptors. *Biochem. Pharmacol.* **50**, 83–90 (1995).
- Devane, W. A. *et al.* Isolation and structure of a brain constituent that binds to the cannabinoid receptor. *Science* **258**, 1946–1949 (1992).
- Dinh, T. P. *et al.* Brain monoglyceride lipase participating in endocannabinoid inactivation. *Proc. Natl Acad. Sci. USA* **99**, 10819–10824 (2002).
- Dinh, T. P., Kathuria, S. & Piomelli, D. RNA interference suggests a primary role for monoacylglycerol lipase in the degradation of the endocannabinoid 2-arachidonoylglycerol. *Mol. Pharmacol.* **66**, 1260–1264 (2004).
- Cravatt, B. F. *et al.* Molecular characterization of an enzyme that degrades neuromodulatory fatty-acid amides. *Nature* **384**, 83–87 (1996).
- Walker, J. M. & Hohmann, A. G. in *Cannabinoids—Handbook of Experimental Pharmacology* (ed. Pertwee, R.) 509–554 (Springer, Berlin, 2005).
- Akil, H., Young, E., Walker, J. M. & Watson, S. J. The many possible roles of opioids and related peptides in stress-induced analgesia. *Ann. NY Acad. Sci.* **467**, 140–153 (1986).
- Herkenham, M. *et al.* Characterization and localization of cannabinoid receptors in rat brain: a quantitative *in vitro* autoradiographic study. *J. Neurosci.* **11**, 563–583 (1991).
- Zimmer, A., Zimmer, A. M., Hohmann, A. G., Herkenham, M. & Bonner, T. I. Increased mortality, hypoactivity, and hypoalgesia in cannabinoid CB<sub>1</sub> receptor knockout mice. *Proc. Natl Acad. Sci. USA* **96**, 5780–5785 (1999).
- Hohmann, A. G., Martin, W. J., Tsou, K. & Walker, J. M. Inhibition of noxious stimulus-evoked activity of spinal cord dorsal horn neurons by the cannabinoid WIN 55,212–2. *Life Sci.* **56**, 2111–2118 (1995).
- Hohmann, A. G., Tsou, K. & Walker, J. M. Cannabinoid suppression of noxious heat-evoked activity in wide dynamic range neurons in the lumbar dorsal horn of the rat. *J. Neurophysiol.* **81**, 575–583 (1999).
- Martin, W. J., Hohmann, A. G. & Walker, J. M. Suppression of noxious stimulus-evoked activity in the ventral posterolateral nucleus of the thalamus by a cannabinoid agonist: correlation between electrophysiological and antinociceptive effects. *J. Neurosci.* **16**, 6601–6611 (1996).
- Meng, I. D., Manning, B. H., Martin, W. J. & Fields, H. L. An analgesia circuit activated by cannabinoids. *Nature* **395**, 381–383 (1998).
- Calignano, A., La Rana, G., Giuffrida, A. & Piomelli, D. Control of pain initiation by endogenous cannabinoids. *Nature* **394**, 277–281 (1998).
- Terman, G. W., Lewis, J. W. & Liebeskind, J. C. Two opioid forms of stress analgesia: studies of tolerance and cross-tolerance. *Brain Res.* **368**, 101–106 (1986).
- Walker, J. M., Huang, S. M., Strangman, N. M., Tsou, K. & Sañudo-Peña, M. C. Pain modulation by release of the endogenous cannabinoid anandamide. *Proc. Natl Acad. Sci. USA* **96**, 12198–12203 (1999).
- Martin, W. J., Patrick, S. L., Coffin, P. O., Tsou, K. & Walker, J. M. An examination of the central sites of action of cannabinoid-induced antinociception in the rat. *Life Sci.* **56**, 2103–2109 (1995).
- Cannon, J. T., Prieto, G. J., Lee, A. & Liebeskind, J. C. Evidence for opioid and non-opioid forms of stimulation-produced analgesia in the rat. *Brain Res.* **243**, 315–321 (1982).
- Tsou, K., Brown, S., Sañudo-Peña, M. C., Mackie, K. & Walker, J. M. Immunohistochemical distribution of cannabinoid CB<sub>1</sub> receptors in the rat central nervous system. *Neuroscience* **83**, 393–411 (1998).
- Kathuria, S. *et al.* Modulation of anxiety through blockade of anandamide hydrolysis. *Nature Med.* **1**, 76–81 (2003).
- Mor, M. *et al.* Cyclohexylcarbamic acid 3'- or 4'-substituted biphenyl-3-yl esters as fatty acid amide hydrolase inhibitors: synthesis, quantitative structure–activity relationships, and molecular modeling studies. *J. Med. Chem.* **47**, 4998–5008 (2004).
- Stella, N., Schweitzer, P. & Piomelli, D. A second endogenous cannabinoid that modulates long-term potentiation. *Nature* **388**, 773–778 (1997).
- Kozak, K. R., Prusakiewicz, J. J. & Marnett, L. J. Oxidative metabolism of endocannabinoids by COX-2. *Curr. Pharm. Des.* **10**, 659–667 (2004).
- De Petrocellis, L., Bisogno, T., Davis, J. B., Pertwee, R. G. & Di Marzo, V. Overlap between the ligand recognition properties of the anandamide transporter and the VR1 vanilloid receptor: inhibitors of anandamide uptake with negligible capsaicin-like activity. *FEBS Lett.* **483**, 52–56 (2000).
- Vaughan, C. W., Connor, M., Bagley, E. E. & Christie, M. J. Actions of

- cannabinoids on membrane properties and synaptic transmission in rat periaqueductal gray neurons *in vitro*. *Mol. Pharmacol.* **57**, 288–295 (2000).
27. Valverde, O., Ledent, C., Beslot, F., Parmentier, M. & Roques, B. P. Reduction of stress-induced analgesia but not of exogenous opioid effects in mice lacking CB1 receptors. *Eur. J. Neurosci.* **12**, 533–539 (2000).
  28. Piomelli, D. The molecular logic of endocannabinoid signalling. *Nature Rev. Neurosci.* **4**, 873–884 (2003).
  29. Tarzia, G. *et al.* Design, synthesis, and structure–activity relationships of alkylcarbamic acid aryl esters, a new class of fatty acid amide hydrolase inhibitors. *J. Med. Chem.* **46**, 2352–2360 (2003).
  30. Giuffrida, A., Rodríguez de Fonseca, F. & Piomelli, D. Quantification of bioactive acylethanolamides in rat plasma by electrospray mass spectrometry. *Anal. Biochem.* **280**, 87–93 (2000).

**Supplementary Information** is linked to the online version of the paper at [www.nature.com/nature](http://www.nature.com/nature).

**Acknowledgements** The assistance of the Centro di Calcolo at the University of Parma is gratefully acknowledged. This research was supported by grants from the National Institute on Drug Abuse (A.G.H., D.P.) and from the MIUR and the Universities of Parma and Urbino ‘Carlo Bo’.

**Author Information** Reprints and permissions information is available at [npg.nature.com/reprintsandpermissions](http://npg.nature.com/reprintsandpermissions). The authors declare competing financial interests: details accompany the paper on [www.nature.com/nature](http://www.nature.com/nature). Correspondence and requests for materials should be addressed to A.G.H. ([ahohmann@uga.edu](mailto:ahohmann@uga.edu)) or D.P. ([piomelli@uci.edu](mailto:piomelli@uci.edu)).